PERGAMON

Deep-Sea Research II 49 (2002) 4115–4130

DEEP-SEA RESEARCH
PART II

www.elsevier.com/locate/dsr2

Physical–biological coupling in the Strait of Gibraltar

Fidel Echevarría[a,*], Jesús García Lafuente[b], Miguel Bruno[c], Gabriel Gorsky[d], Madeleine Goutx[e], Nicolás González[f], Carlos M. García[a], Fernando Gómez[a], Juan M. Vargas[b], Marc Picheral[d], Laurent Striby[e], Manuel Varela[f], Jose J. Alonso[c], Andreas Reul[g], Andrés Cózar[a], Laura Prieto[a], Tarek Sarhan[b], Francisco Plaza[b], Francisco Jiménez-Gómez[h]

[a] *Area de Ecología, Facultad de Ciencias del Mar, Universidad de Cádiz, 11510 Puerto Real, Cádiz, Spain*
[b] *Departamento de Física Aplicada II. Universidad de Málaga. Campus de Teatinos. 29071 Málaga, Spain*
[c] *Departamento de Física Aplicada, Facultad de Ciencias del Mar, Universidad de Cádiz, 11510 Puerto Real, Cádiz, Spain*
[d] *Laboratoire d'Oceanographie Biologique et Ecologie du Plancton Marin, Station Zoologique, 06234 Villefranche sur Mer, France*
[e] *Laboratoire de Microbiologie Marine, CNRS/INSU-EP2032, Universite de la Mediterranee, Campus de Luminy, Case 907, Marseille Cedex 9, France*
[f] *Instituto Español de Oceanografía, Muelle de Animas s/n, 15001 A Coruña, Spain*
[g] *Departamento de Ecología. Universidad de Málaga. Campus de Teatinos. 29071 Malaga, Spain*
[h] *Departamento de Biología Animal, Vegetal y Ecología. Universidad de Jaen. Paraje Las Lagunillas s/n. 23071 Jaen, Spain*

Received 28 April 2000; received in revised form 28 March 2001; accepted 17 July 2001

Abstract

This study presents a joint analysis of the distributions of some biogeochemical variables and their relation to the hydrodynamics of Gibraltar Strait. It is a synthesis paper that brings together many results obtained during CANIGO project. We show the role of hydrodynamics as a forcing agent for the plankton community structure in the Strait, with emphasis on the two physical processes that we propose as key factors for the coupling: interface position and oscillations, and mixing processes along the Strait. As a general pattern, autotrophic plankton biomass increases at the Strait from southwest to northeast, a tendency that coincides with a gradual elevation of the interface depth in the same direction. The different mechanisms of mixing that take place in the Strait are briefly reviewed: The occurrence of the internal hydraulic jump is an important mechanism of mixing constrained to the spring tide situations, but other processes such as the generation of arrested internal waves of wavelength around 1 km are proposed as a complementary mixing mechanism, particularly during neap tides situations. Both mechanisms, the elevation of the pycnocline and these mixing events, can enhance biological productivity and biomass accumulation on the northeastern sector of the Strait, since phytoplankton cells are there packaged in a water mass with sufficient light and nutrients and smaller advective velocity. There is a clear north–south difference in the biological response to these upwelling episodes in the eastern section, with high nutrient and low chlorophyll in the south and the opposite in the north. The deeper interface and the greater water speed are the proposed reasons for this lower nutrient uptake on the southeastern sector. Finally, the temporal scales of variation of the mixing events, the influence of its periodicity on the productivity of the area and the influence of these upwelling episodes in the nearest Alborán Sea are discussed.

*Corresponding author. Tel.: +34-956-01-6025; fax: +34-956-01-6019.
E-mail address: fidel.echevarria@uca.es (F. Echevarría).

0967-0645/02/$ - see front matter
PII: S0967-0645(02)00145-5

1. Introduction

The Strait of Gibraltar is the narrow and shallow connection between the Mediterranean Sea and the Atlantic Ocean, with a minimum width of about 14 km and a sill depth of about 300 m. The water circulation in the Strait is characterised by a surface inflow of Atlantic waters and a deep outflow of dense Mediterranean water, which is ultimately driven by the excess of evaporation over precipitation in this basin (see Lacombe and Richez, 1982, for instance). According to Bryden et al. (1994), the exchanged flows at the sill, the section of minimum cross-area, are of the order of 0.7 Sv, ($1\,\mathrm{Sv} = 10^6\,\mathrm{m^3\,s^{-1}}$) with a net flow into the Mediterranean of around 0.05 Sv necessary to balance the evaporative losses. The description of the exchange as a simple one-dimensional, two-layer system flowing in opposite directions is a good first approximation (Armi and Farmer, 1988), but it is deficient in describing the vertical structure of some variables and their changes across and along the Strait.

A variety of phenomena are superposed on, and interact with, this basic inverse estuarine circulation (e.g., Armi and Farmer, 1988). Transport fluctuations at tidal and longer periods can reverse the flows. At spring tides, in particular, an internal bore tends to be released from the sill as the tide reverses from ebb to flood, this bore breaking up into a series of large internal waves (Alpers et al., 1996). Important mixing can accompany the large-amplitude internal motions (Wesson and Gregg, 1994). Recently, other processes producing mixing also during neap tides has been identified (Bruno et al., 2002). The effect of these mixing mechanisms on the biology is explored in this paper.

Research in biological oceanography at the Strait has been very scarce. There are some estimations of different biogeochemical variables sampled in surveys with large spatial grid and not specifically designed to investigate the Gibraltar area itself, and without an analysis aimed to connect the distribution of these variables and hydrodynamics. During the MEDIPROD IV survey (October–November 1981), the interpretation of some biological and geochemical distributions was made from the standpoint of very general principles of the physical oceanography (i.e. Packard et al., 1988; Minas et al., 1991), with emphasis in the Mediterranean sector of the Strait and without a detailed study of the biological communities.

Within CANIGO, a large set of physical and biogeochemical observations was collected in order to carry out an analysis of the influence of the physical structure on the distribution of nutrients, organisms, and particles. Preliminary observations of the distribution of some diatom species led us to propose a re-circulation model or a conveyor-belt-like system drawn by the two-layer structure of the Strait (Gómez et al., 2000a). Efforts also were done during CANIGO to estimate the fluxes of several materials through the strait (e.g. Gómez et al. (2000b), for nutrient fluxes; Dafner et al. (2001), for organic and inorganic carbon fluxes; Elbaz-Poulichet et al. (2001), for metal fluxes; Reul et al. (2002), for biomass fluxes).

Here, we synthesise information split between several works (Bruno et al., 2002; García Lafuente et al., 2000; García Lafuente et al., 2002; Gómez et al., 2000a, b; Reul et al., 2002) to show the role of hydrodynamics as a forcing agent for the plankton community structure and associated water chemistry in the Strait of Gibraltar. First, we describe the main oceanographic features at the Strait, with emphasis on the two physical processes that we propose as key factors for the coupling: the interface position and oscillations, and the mixing processes along the Strait, especially at the sill area. Then, we analyse the mechanisms involved in the suggested coupling given the response of organisms to these physical phenomena.

2. Methods

During two cruises on board R/V *Cornide de Saavedra* (June 18–25, 1997) and R/V *Thalassa* (September 2–9, 1997), we sampled eight stations arranged in three transects at the Atlantic, Central and Mediterranean sections of the Strait (Fig. 1). The stations were repeatedly sampled during a semidiurnal tidal cycle at a variable sampling

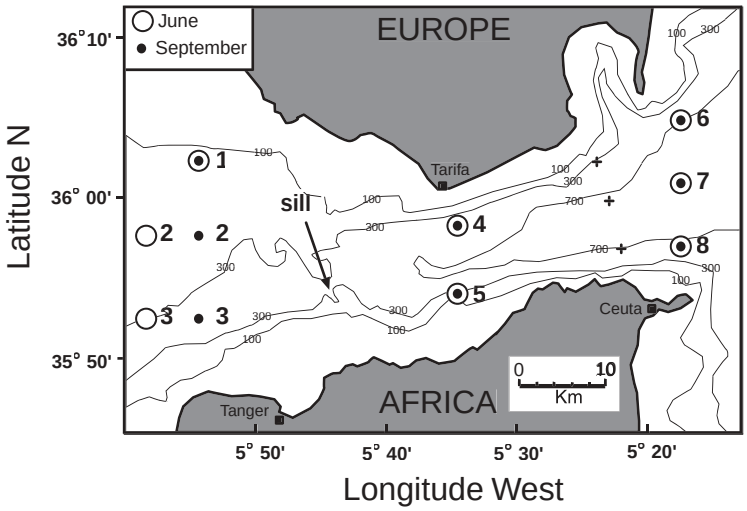

Fig. 1. Map of the Strait of Gibraltar, showing the bathimetry and the position of the sampling stations at June (open circles) and September (filled circles). Crosses represent the position of the three mooring lines with currentmeters. The Camarinal Sill position is also shown.

interval that ranged between 1 and 3 h. Finally, we include observations made at the sill area of the Strait (Fig. 1) on board R/V *Investigador* in November 1998, an opportunity ship equipped with ADCP and a CTD with an additional sensor of transmissivity. The details of this last cruise are given in Bruno et al. (2002). Other observations from a mooring array deployed at the eastern section of the Strait (see Fig. 1; García Lafuente et al., 2002) also have been used.

During the CANIGO cruises water samples were collected with a CTD-rosette outfitted with 20-l Niskin bottles. Also, several Underwater Video Profiler (UVP) (Gorsky et al., 2000) casts were performed at each station. This multisensor included CTD, fluorometer, nephelometer (turbidity measurements), and a video system for the abundance and size assessment of particles $>500\,\mu m$. These large particles (marine snow) were filmed by a video camera and analysed by an automatic image analyser (Gorsky et al., 2000, Stemmann et al., 2000).

Samples of dissolved inorganic nutrients (5 ml) taken at the different sampling depths were frozen ($-20^{\circ}C$). After thawing, concentration of nitrate was measured with an automatic Technicon AA-II analyser following the method described by Grasshoff et al. (1983). For total chlorophyll a concentration, 500 ml of seawater were filtered through Whatman GF/F glass fibre filters and chlorophyll was extracted in a 90% acetone solution overnight (UNESCO, 1994). Fluorescence was measured in a Turner Designs-10 fluorometer. To estimate the concentration of chlorophyll $>20\,\mu m$, 2.5 l of water were filtered through a 20 μm pore size mesh.

For microplankton analysis, 2 l of water were filtered through a 5-μm pore sized mesh and the retained material was preserved with Lugol's solution. Subsamples (10–50 ml) were settled in Utermohl chambers and counted with an inverted microscope. Simultaneously to the counting process, microplankton biomass expressed as biovolume was calculated by approximation to regular figures (ellipsoid, cylinder, hemisphere) using a VIDS V (Analytical Measuring Systems, Inc.) semiautomatic image analysis system. Abundance of smaller size categories of plankton was estimated by using flow cytometry.

2.1. Interface definition

The conveyor-belt biophysical model previously suggested for the Strait (Gómez et al., 2000a) has a

time scale related to the time it takes a water parcel in the upper layer (lower layer) to travel from the Camarinal sill to the eastern section of the Strait, which are a distance of about 40 km. For a spatially averaged typical inflowing velocity of $0.5\,m\,s^{-1}$, this time is 1 day, while the time it takes a water parcel in the lower layer to move the opposite way is somewhat longer because of the slower outflowing velocity. Tidal velocities may modify these times slightly. Thus, the time scale of interest is from several hours to several days.

At these time scales, tidal fluctuations dominate the flow variability. Tidal transports are two or three times greater than the time-averaged transport (Bryden et al., 1994; García Lafuente et al., 2000). Consequently, the flow of one of the layers reverses in some places of the Strait during some periods of the tidal cycle (Candela et al., 1990; Bryden et al., 1994; García Lafuente et al., 2000), and the entire water column moves in the same direction. When this unidirectional flow happens, the two-way exchange interface, which separates inflow and outflow, disappears. However, from the standpoint of water mass characteristics the interface still exists and it must be defined in terms of these characteristics. Due to mixing, this hypothetical interface actually becomes a mixing interfacial layer separating purer Atlantic and Mediterranean waters. In order to characterise this mixing-layer we have followed a method similar to that used by Bray et al. (1995). It consists of fitting a "smooth two layer function" of the form

$$S(z) = \frac{S_2 - S_1}{1 + \exp\left(\frac{z - z_0}{\Delta z}\right)} + S_1$$

to the observed salinity profiles. Here, z is the depth, and S_1, S_2, z_0 and Δz are parameters to be estimated. S_1 and S_2 can be identified with the salinity of the Atlantic and Mediterranean layers in a two-layer system, z_0 is the depth of the midpoint of the halocline (and of the maximum salinity gradient, as well), which would correspond to the depth of the interface in a two-layer system, and $6\times\Delta z$ is the halocline thickness that we identify with the mixing-layer thickness. The quality coefficient of the fitting, defined in the same way as in Bray et al (1995), was greater than 0.9 in 184 out of 222, fits and only in 11 cases it was less than 0.7. Therefore, the fitting is good and explains more than 90% of the variance of the original data on average.

3. Results and discussion

3.1. The position of the interface

Figs. 2A and B show the spatial distribution of z_0 (i.e. of the interface) during both cruises. It agrees well with the classically reported interface shape in the Strait, showing the along-strait gradient, typical of a density driven two-layer flow, and the across-strait gradient forced by the earth rotation. The surface of null along-strait velocity that is well defined for slowly varying subinertial flows (García Lafuente et al, 2002) must lay somewhere within this mixing layer (an example of this feature can be seen in Fig. 3 of Reul et al., 2002). Therefore, our definition of the interfacial mixing layer is consistent with the stricter definition used in studies of low frequency variability of the steady exchange.

The combination of the aforementioned gradients produces a shallower interface at the northeastern side of the Strait. Figs. 2C and D show the thickness of the mixing layer in June and September, respectively. It is thicker in the south and thinner in the north, with the northeastern part of the Strait being the place with the thinnest mixing layer. Globally, this layer was thicker in September than in June and the along-strait slope was noticeably steeper in June. These differences are not surprising if we consider the important subinertial variability of the exchange through the Strait (Candela et al., 1989).

The method followed to determine the interface and the mixing layer has the advantage of describing these important parameters taking into account the local properties of the water column. We can easily determine which value of salinity corresponds to z_0 at each station, and use this value to decide if a given sample was acquired in the upper or in the lower layer. In other words, if S_0 is the local salinity in $z_0(x, y)$, then a biological

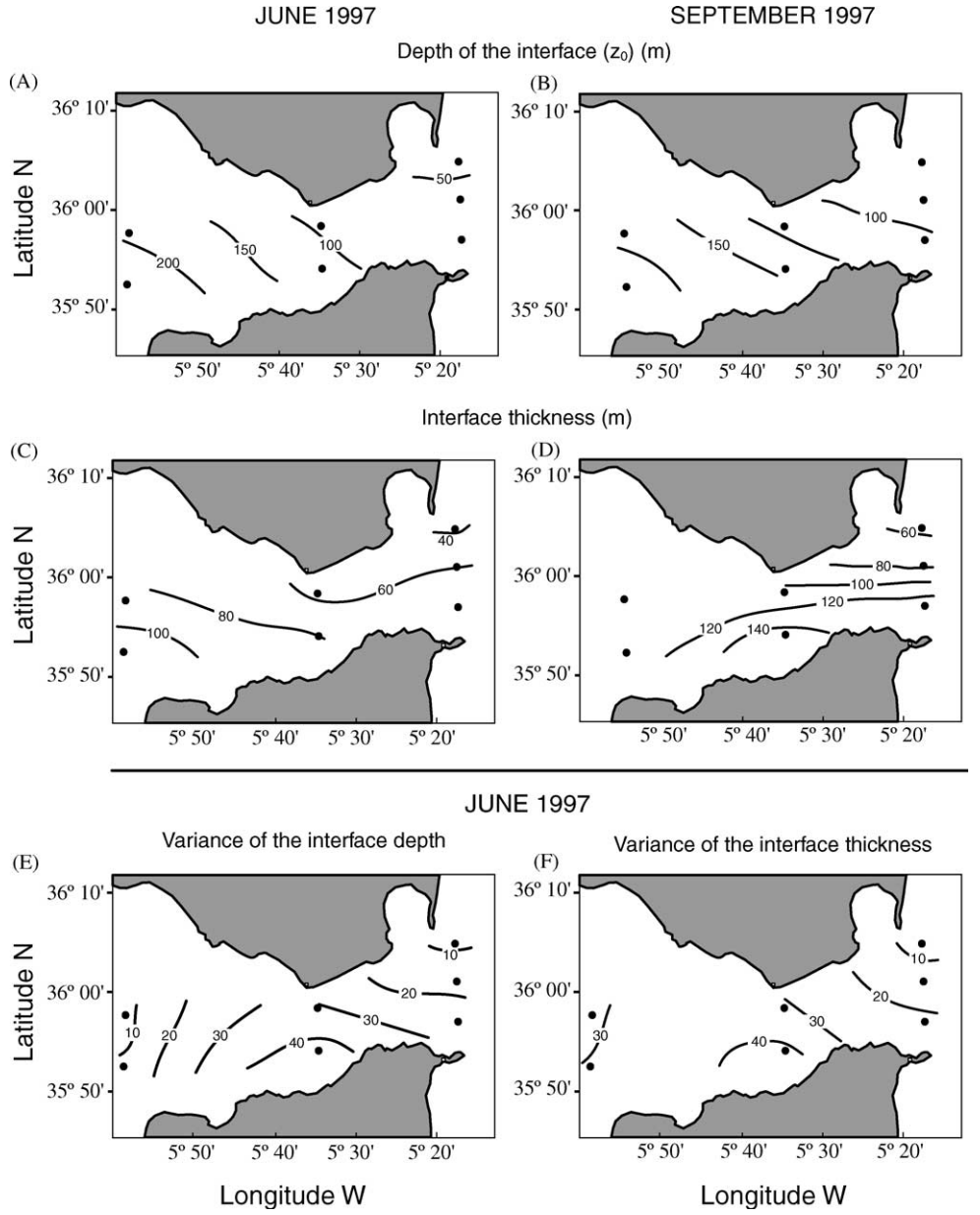

Fig. 2. (a,b) Maps of the mean interface depth (m) defined as the mean value of z_0 (see text) for all the CTD casts accomplished at each station during the cruises of June and September, respectively. (c,d) Maps of the mean interface thickness (m) defined as the mean value of $6 \times \Delta z$ (see text) for all the CTD casts accomplished at each station during the cruises of June and September, respectively. (e) Variance (m^2) of the mean interface depth during June (that is, variance of the variable in (a)). (f) Variance (m^2) of the mean interface thickness during June (that is, variance of the variable in (c)).

sample collected in point $[x, y, z]$ is considered as belonging to the upper (lower) layer if the salinity $S(x, y, z)$ at this point is less (greater) than S_0. All vertical salinity profiles collected verified that wherever $S(x, y, z)$ was less (greater) than $S_0(z_0(x, y))$, z was above (below) $z_0(x, y)$. This

Table 1
Depth of the interface, thickness of the interfacial mixing layer, and salinity at the depth of the interface (see text for details) during both cruises

St.	June			September		
	z_0	$6 \times \Delta z$	S_0	z_0	$6 \times \Delta z$	S_0
2	185	90	37.18	170	100	37.35
3	230	110	37.28	195	115	37.30
4	65	55	37.27	110	105	37.42
5	135	80	37.35	150	145	37.40
6	35	40	37.80	80	55	37.63
7	60	60	37.46	90	80	37.56
8	70	70	37.40	105	125	37.56

additional test is necessary to ensure the correctness of the criterion because salinity does not increase monotonically with depth (small salinity inversions are often found in the upper layer of the Strait because of the presence of North Atlantic Central Water, NACW). Table 1 shows the values of $S_0(x, y)$ for the different stations, which agree with the values reported in the literature (Bryden et al., 1994; García Lafuente et al., 2000). The importance of this criterion is evident in order to identify the layer to which a biological sample belongs.

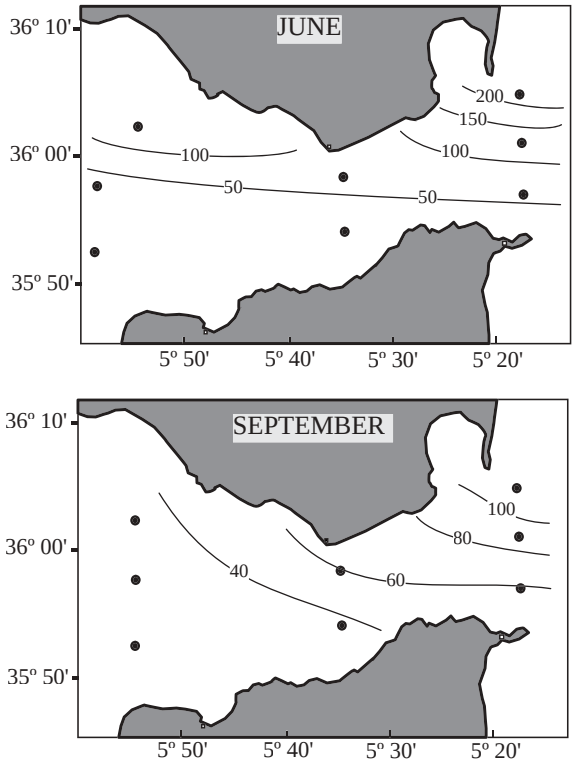

Fig. 3. Integrated chlorophyll distribution ($mg\,m^{-2}$) for the upper 100 m at both CANIGO cruises.

3.2. Distribution of biomass and particles

Our results show a relevant role of interface position and oscillations explaining the biomass distribution pattern. The depth-integrated chlorophyll values at the 8 stations sampled at both cruises (June and September) are plotted in Fig. 3. A clear general increase towards the northeast can be found, an increase, which parallels the interface ascent. Similar tendencies have been found for the two cruises performed, although June chlorophyll patterns show higher spatial heterogeneity and a more marked N–S gradient than in September. This is especially clear in the eastern section of the Strait. The tidal phase when stations were sampled can have an influence on the variability; found, thus in June almost all the stations were sampled near HW (high-water), whereas in September the stations placed on the main SW–NE axis were visited near LW (low-water). Another temporal difference is that station 1 showed high variability between both sampling periods. The shallowness of this coastal station ($\sim$150 m depth) favours the appearance of events that lead to an enhanced production (Establier and Margalef, 1964).

The distribution of chlorophyll and microphytoplankton is affected by the depth of the interface, which shows a clear ascent towards the northeast. But also the position of the thermocline and the separation between the two discontinuities, thermocline and interface, affect these distributions: In the Atlantic side, the thermocline is more than 100 m shallower than the interface, the chlorophyll showing subsurface maxima associated with the thermocline. Northeastwards, the interface rises and gradually merges with the thermocline in a shallow position. This coincidence reinforces the stratification and can enhance the chlorophyll-rich area observed. The magnitude

of the chlorophyll value is inversely related to the distance between the interface and the thermocline, a fact previously reported by Rodríguez et al. (1998) in a frontal region in the adjacent Alborán Sea. The contribution of chlorophyll > 20 μm to total chlorophyll also differs between Atlantic and Mediterranean waters (Fig. 5C). Around 40% of total chlorophyll corresponds to the fraction of cells > 20 μm in NE stations whereas only less than 10% of total chlorophyll belongs to cells larger than 20 μm in the Atlantic transect (specially at the southern station). Therefore, there is a difference in the predominant sizes and species of phytoplankton cells, with larger cells occurring preferentially in the Mediterranean stations of the Strait. This fact is not surprising as the selection of size and shape of phytoplankton species that leads to the observed assemblages structure have been classically related both to nutrient and turbulent energy levels (Margalef, 1978) and recently to vertical velocities (Rodríguez et al., 2001). Indeed, the smaller size fractions of picoplankton (0.2–2 μm) and nanoplankton (0.2–2 μm) behave in a different manner, with higher concentrations at the Atlantic side (Reul et al., 2002).

Although casts were not coincident with water sampling, the results from the Underwater Video Profiler fit well with the distribution of phytoplankton (Figs. 4 and 5). In the Mediterranean side, the high concentration of phytoplankton is correlated to the concentration of large particles (> 500 μm) and turbidity (particles < 50 μm). The distribution of turbidity along the Strait shows the same pattern described by Jerlov (1953). This author reported high-turbid waters located in the upper layer of the Mediterranean entrance of the Strait (associated with high phytoplankton biomass) and near the bottom of the Atlantic entrance (associated with the Mediterranean Outflowing Waters—MOW) (Fig. 4 in Jerlov, 1953). However, the deep Mediterranean current presented low values of turbidity before crossing the sill (Mediterranean side). The minimum value of turbidity reported by Jerlov (1953) coincided with the NACW layer in the Gulf of Cadiz. The lower values of turbidity observed in the NACW in comparison with the Surface Atlantic Water (SAW) could be related to the position of the NACW in the stratified water column in the Gulf of Cadiz. If we consider that the distribution of suspended matter is closely related to the production of living matter, the SAW (in the euphotic zone) could present high concentration of small particles originated from biological activity. In contrast, NACW (aphotic zone) presents low particle values that depend on the fallout from the overlying SAW. Although the concentration of particles in the NACW increased along the Strait, it did not reach the values observed in the SAW.

The biological similarity between upper layers of Mediterranean stations and lower layers of central (and sometimes Atlantic) stations could indicate advective connections between the stations (Figs. 4 and 5). This similarity also is supported by the distribution of the main taxonomic groups of microphytoplankton. Phytoplankton assemblages are very similar in central and Mediterranean stations; both placed at the same side of Camarinal Sill. The microphytoplankton assemblage at these stations is dominated by diatoms, mainly the genera *Chaetoceros*, *Guinardia,* and *Rhizosolenia*, and is very different to the phytoplankton assemblage typical of the Atlantic sector, on the other side of the sill, with a dominance of dinoflagellates and relatively more microheterotrophs (Gómez et al., 2000a). These differences match well with the consideration of eutrophic conditions toward the east and oligotrophic to the west of the Sill. To explain the differences in the community structure found on either side of the Sill, it is important to take into account the mixing processes that take place along the Strait, but especially at the Camarinal Sill region. We review this subject in the following section.

3.3. Mixing processes in the Strait

Mixing is a key issue in the conveyor-belt scheme. It is responsible for the degeneration of the interface into an interfacial mixing layer, thus contributing to the enrichment processes of the upper layer. There are several sources of mixing associated with the different time scales of the flow variability. The first one is related to the sheared vertical structure of the mean flow, which is more important in those zones where the spatial

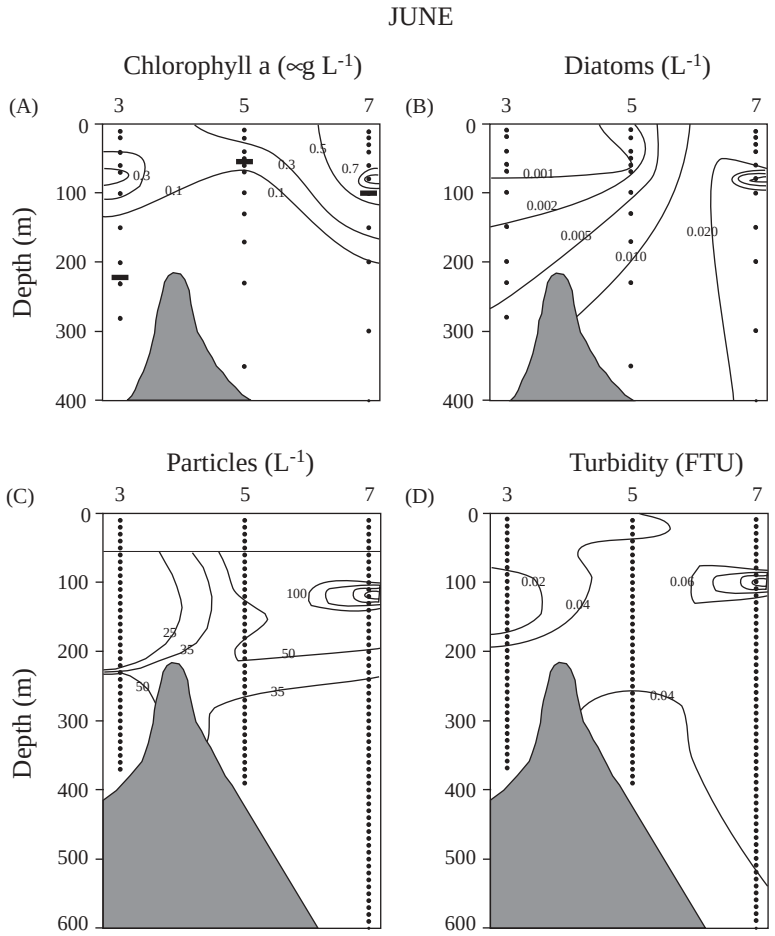

Fig. 4. Along-strait vertical distribution of (A) chlorophyll *a* ($\mu g\,l^{-1}$), (B) diatoms concentration ($cells\,l^{-1}$), both down to 400 m. (C) particles (No. l^{-1}) and turbidity (FTU) down to 700 m during the June cruise. Stations 3, 5 and 7 have been selected because they are aligned along the main channel. Note the instantaneous position of the Atlantic–Mediterranean Interface as a horizontal thick line in the upper profiles.

acceleration of the flow is high. East of Camarinal Sill, the inflow accelerates and entrains water from the lower layer. The interfacial layer moves, on average, toward the east driven by this mechanism (Bray et al., 1995). A consequence is that the amount of inflow and outflow at the eastern section is greater than at the sill section, which implies upward motion from the lower layer to conserve mass.

A second source is tidal in origin, particularly associated with the semidiurnal M_2 tide, which is the main source of flow variability (see, for instance, Candela et al., 1990). Tidal flow is strongly dependent on the along-strait coordinate. García Lafuente et al. (2000) reported a M_2 inflow signal of 0.3 Sv at the eastern section, while Bryden et al. (1994) calculated 2.3 Sv at Camarinal Sill. The difference must remain in between (internal divergence), feeding a fluctuating reservoir and making the interface to oscillate up and down. Important mixing is expected to occur in this reservoir, which is associated with the baroclinic nature of the tidal motions. Also, the thickness of the interface is sensitive to this dynamics since

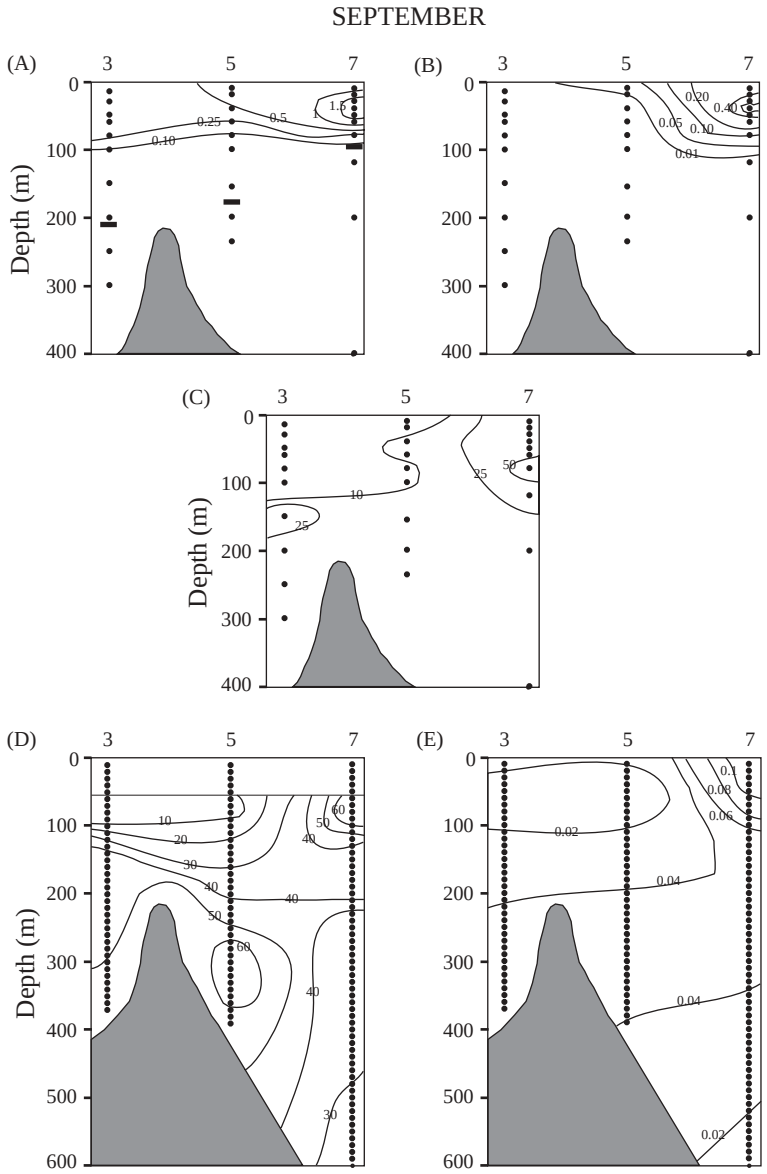

Fig. 5. Along-strait vertical distribution during the September cruise: (A) chlorophyll a ($\mu g\,l^{-1}$), (B) diatoms concentration (cells l^{-1}), (C) percentage of chlorophyll in cells larger than 20 μm, (D) particles (No. l^{-1}) and (E) turbidity (FTU).

mixing is enhanced during flood tide when the vertical shear of horizontal velocity is greater (García Lafuente et al., 2000). The series of CTD casts accomplished during both CANIGO cruises allow us to roughly depict these features. Figs. 2E and F show the variance of the interface depth (z_0) and interface thickness (Δz) during June. The sill area is the place with the greatest variance of both parameters. Also, a clear south to north gradient is observed at the eastern section, suggesting that internal tidal dynamics is enhanced in the south.

A third and more important source is linked to processes occurring at subtidal time scales, such as the periodic formation during flood tide (westward flow) of internal hydraulic jumps west of Camarinal Sill and their subsequent release (Armi and Farmer, 1988). These authors showed the existence of fine structure in the salinity and temperature profiles taken in the jump, which is indicative of active mixing. Another short time-scale internal process producing significant mixing is the generation of arrested internal waves over the Camarinal Sill crest during some flood tides, whose wavelength is around 1 km (Bruno at al., 2002). The interaction of the velocity profile of the wave and the basic flow increases the velocity shear in the wave trough, enhancing the interfacial mixing, as suggested by the fine structure visible in the vertical profiles of salinity and temperature taken in the trough of one of these waves (see Fig. 6 of Bruno et al., 2002). Figs. 6A–C illustrate the coupling between the wave shape (determined by the position of the isohalines), the vertical velocity, and the concentration of particulate material measured by the transmissometer. The

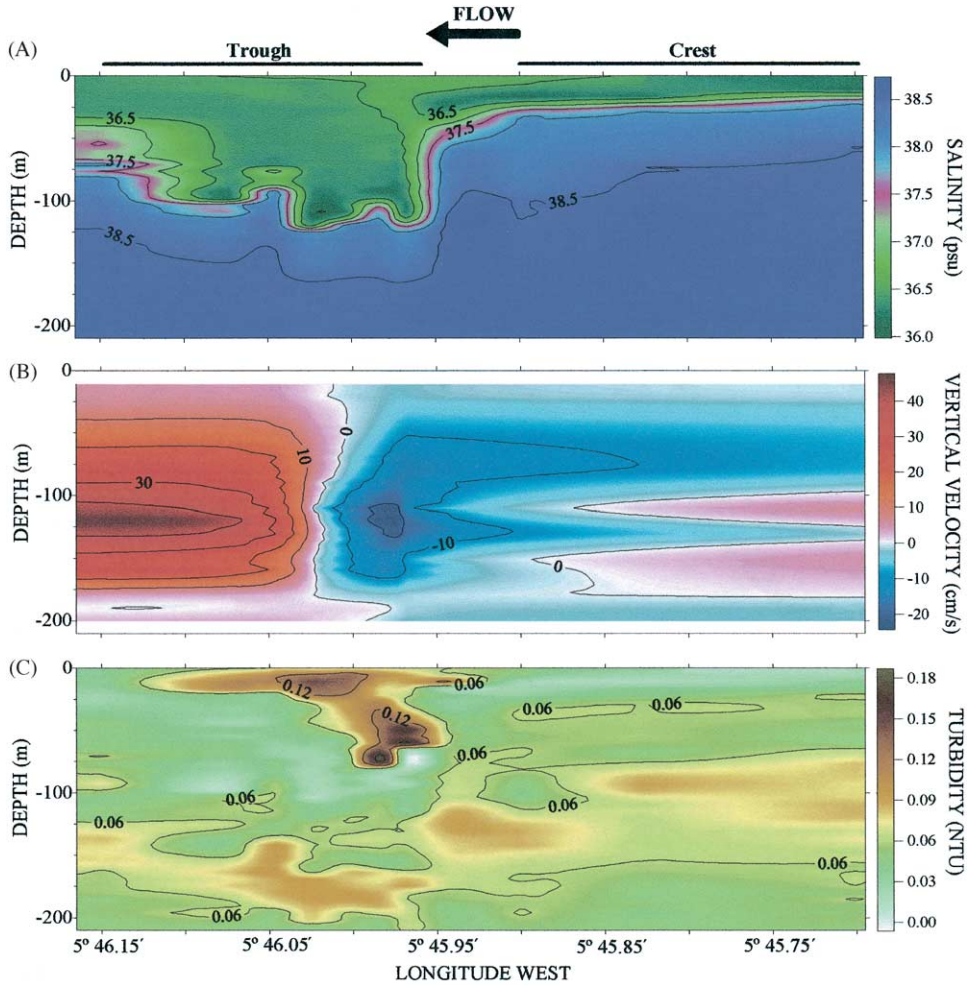

Fig. 6. Contour plot of salinity (a), vertical velocity (b), and turbidity (c) during an "arrested wave" episode at the sill region of the Strait.

vertical velocity has the expected pattern for a wave that has tendency to propagate toward the east but that remains arrested by the flow. The particulate material is concentrated in the wave trough as a consequence of vertical advection by the velocity wave field. Further mixing would spread this material and fertilise the upper layer. The details of the sampling and analysis of the arrested wave event presented in Fig. 6 can be found at Bruno et al. (2002).

These two processes are mutually exclusive. Trapping of the waves always occurs under subcritical conditions over Camarinal Sill when the internal Froude number ($G^2 = [u_1^2/g'h_1] + [u_2^2/g'h_2]$, where u_i and h_i, $i = 1, 2$, are the velocity and thickness of layer i, respectively, and g' is the reduced gravity) is 0.6–0.7 (Farmer and Armi, 1999). The internal hydraulic jump needs critical condition at the sill ($G^2 = 1$). Since $G^2 < 1$ is associated with weaker tidal flows, the formation of arrested waves is more frequent during neap tides and appears to be the replacing mixing mechanism of the hydraulic jump. In both cases, when the flood tide slacks, the waves or the internal jump are released, facilitating the advection of the material previously pumped by the wave or the jump to the east. Further mixing in the leading border of the released wave trains or internal bore is expected to happen during its subsequent eastward propagation. For G^2 greater than 0.7, however, no arrested waves were observed (Bruno et al., 2002) and the interval $0.7 < G^2 < 1$ is not adequate for mixing processes associated with these hydrodynamic features. $G^2 < 0.6$ leads to neither the generation of arrested waves nor to the hydraulic jump, so that mixing at Camarinal Sill is greatly reduced.

All these processes, particularly the arrested waves and the hydraulic jump, are effective mixing mechanisms, though they are difficult to quantify. Wesson and Gregg (1994) estimated the mixing between both layers to be about 0.1 Sv, which is a significant percentage of the outflow.

3.4. Nutrients and plankton response to mixing

Nitrate concentrations along the Strait (st. 3, 5, 7) are shown in Figs. 7A and B, with similar trends found at June and September cruises. On the Atlantic side, the interface is deeper and the nitrate concentration in the upper layer is low. In the central station the nitrate concentration in the upper layer increases, regardless of the depth of the interface, which was significantly different during both cruises. The mixing events at the sill region previously discussed should be the reason for this increase in nutrient concentration. During the eastwards displacement of upper water this nutrient could be progressively consumed by phytoplankton, as is suggested by the lower concentration in the Mediterranean side (st. 7).

Minas et al. (1991) have previously proposed the influence of mixing events at the sill. These authors showed the highest nutrient concentration of the Mediterranean at the middle of the Strait as a consequence of these mixing events. However, it is uncertain the amount of nutrient recovered by vertical mixing through the interface and the incidence of the injection of nutrient-rich North Atlantic Central Water at the sill (Minas and Minas, 1993).

When mixing events occur at the sill region of the Strait, the surface water enriched with nutrients is advected towards the Mediterranean, with decrease of nutrients and an increase of chlorophyll (Figs. 4, 5 and 7). Mixing processes described in the previous section imply significant recirculation of Mediterranean waters, which affects the surface nutrient concentration, and propitiates the ascent of seeding cells. Gómez et al. (2000b) proposed a potential value of $40\,\mathrm{kg\,C\,s^{-1}}$ as a preliminary estimation of the contribution of the upwelled nutrients (estimated in $500\,\mathrm{mol\,NO_3\,s^{-1}}$, taking the value of 0.1 Sv of upwelled water mentioned by Wesson and Gregg (1994) and a NO_3 concentration of $5\,\mu\mathrm{mol\,l^{-1}}$) to plankton biomass, assuming the constant 1.59 to convert mmol nitrate to mg Chl a (Takahashi et al., 1986), a carbon to chlorophyll ratio of 50 (Harris, 1986), and the Redfield ratio (C:N = 6.6).

However, there is a clear north–south difference in the plankton response to this enrichment. The increase of chlorophyll occurs only in the north (st. 6 and 7) while it does not occur in the south (st 8) (Fig. 3). Nutrients are low in the north, probably because of phytoplankton uptake, and are highest

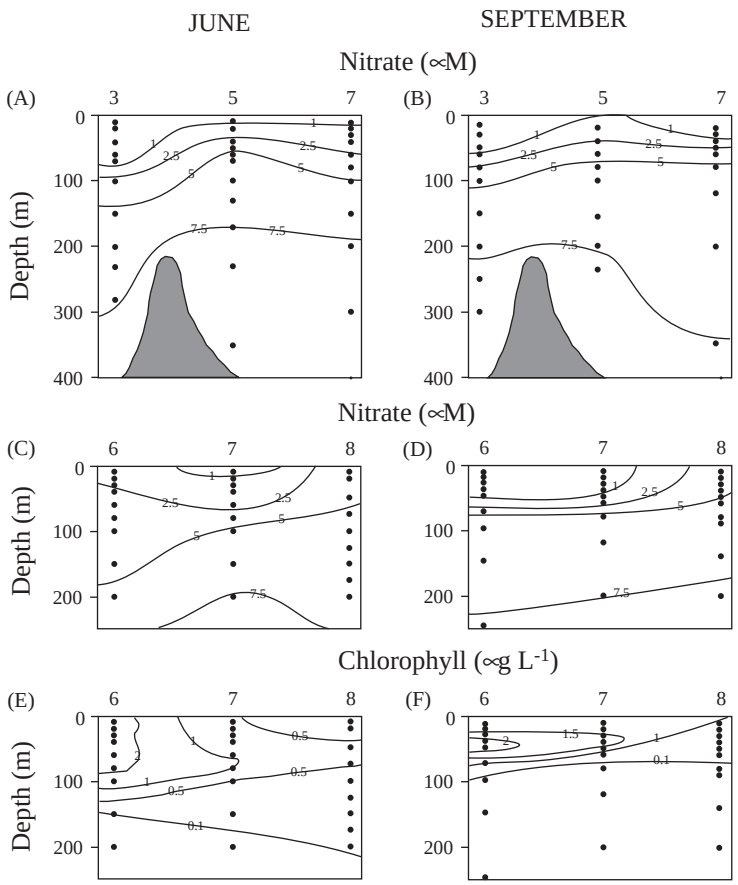

Fig. 7. (Upper panels) Along-strait (st. 3, 5, 7) vertical distribution of NO_3 during June and September cruises. (Central panels) Across-strait vertical distribution of NO_3 at the eastern section of the strait (st. 6,7,8) during June and September cruises. (Lower panels) Across-strait vertical distribution of chlorophyll at the same eastern section of the Strait.

in the SE (st 8). To explain this different N–S response, there are two variables that change significantly in this across strait direction and must be taken into account: interface depth and water velocity.

On the eastern side of the Strait the average interface is shallower towards the north (Fig. 2). In the upper layer of the station 6, the low nutrient concentrations could be attributed to the high phytoplankton abundance, although in June, the proximity of the interface to the surface alters the general trend. In the Station 8, on the southeastern side, we found the highest concentration of nitrate at both cruises, together with lower chlorophyll values (Fig. 7). Station 8 also must receive the upwelled nutrients from the sill region, but phytoplankton does not incorporate these nutrients which may be due to the fact that the interface is deeper. Also, it does not coincide with thermocline. We could relate these patterns to the Sverdrup effect, which can be described as the enhancement in productivity that occurs when an episode of mixing is followed by stratification shallow enough to confine the cells in a well-illuminated layer (i.e. Mann and Lazier, 1991). Sverdrup (1953) introduced the concept of ''critical depth'' as the depth at which the integrated (through depth and time) gross photosynthesis equals the integrated respiration by phytoplankton. If there is no nutrient limitation and the depth

of mixing is less than the critical depth, integrated gross photosynthesis is larger than integrated respiration, and net production will result.

The horizontal water velocity also has important across-strait structure (Pettigrew and Hyde, 1990; Fig. 3 of Reul et al., 2002). Mean inflowing velocities increase from $\sim 40\,\mathrm{cm\,s^{-1}}$ in the north to $\sim 75\,\mathrm{cm\,s^{-1}}$ in the south. The depth of the null along-strait velocity of the mean exchange deepens from 100 m at the north mooring to 130 m at the south (see Fig. 3 of Reul et al., 2002). Both features would produce a mean transport per width unit around 2.5 times greater in the south than in the north. This across-strait structure of the flow influences the spatial distribution of biological variables. For instance, if we assume that the aforementioned nutrient fertilisation of the upper layer in Camarinal Sill is spatially homogeneous, then the nutrient flux on the eastern section would be around 2.5 times higher at the southern part of the Strait. In addition, the faster inflowing velocity in the south implies that microphytoplankton has less time to convert nutrients into biomass. Thus, the $40\,\mathrm{kg\,C\,s^{-1}}$ of total biomass generated at the Strait proposed by Gómez et al. (2000b) should be an overestimation if taking only into account the northern half eastern cross-section of the Strait as the place in which the nutrients upwelled are converted into biomass.

The across strait slope of the interface makes the biomass to lie closer to the interface, and hence to the zero-velocity layer, in the north than in the south at the eastern Mediterranean stations. This facilitates the biomass accumulation and prevents the cells from being advected quickly into the Alboran Sea: repositioning in the water column due to changes in buoyancy is usually found in microphytoplankton cells (Smayda, 1970). The advantages of this ability becomes noteworthy in this particular situation, since a population in the vicinity of the interface experiences a diminished eastward speed and, simultaneously, a more continuous nutrient supply.

Recently, we have proposed the countercurrent system of the Strait as a conveyor-belt scheme to which some diatoms species could couple their life cycles (Gómez et al., 2000a). This scheme would allow the diatoms in the surface waters of the eastern side of the Strait to aggregate and to sink below the interface, with resting or less active propagules moving westwards and a part of the population returning to the surface waters by means of the mixing of deep Mediterranean water at the sill. This mechanism could contribute to maintain both high biomass values in the Mediterranean side of the Strait and taxonomic similarities among these stations. Nevertheless, this hypothesis needs further validation through field analysis.

3.5. Temporal variation of mixing phenomena

Mixing phenomena in the Strait occur at a diversity of time-scales. The fortnightly cycle is responsible for two types of phenomena that influence the mixing. On one hand, spring tides are the times of the highest probability of formation of large internal hydraulic jumps west of Camarinal Sill (Armi and Farmer, 1988). Mixing in the jump and in the internal travelling bore after the jump's release, would produce a thicker interfacial or mixing layer. In addition, the vertical shear of horizontal velocities is increased since tidal velocities are higher. García Lafuente et al. (2000) show a clear fortnightly signal in the thickness of the interfacial layer at the eastern section, with maximum thickness one day after new or full moon, according to the aforementioned comments. Out of spring tides the hydraulic jump can be replaced by the topographically arrested wave, which is another important mechanism for mixing and pumping nutrients into the euphotic zone.

Although more observations are needed to elucidate the ranking of importance of these two mixing mechanisms, it seems that the internal hydraulic jump is more efficient. The jump is the mechanism by which the kinetic energy of the flow transforms into turbulent (and potential) energy to adjust the energetic supercritical flow upstream of the jump to subcritical flow downstream. The arrested wave does not undergo such adjustment, so that turbulence would be less. Therefore, mixing would be enhanced in spring tides and the proposed mechanism of coupling would find better

conditions during spring tides than during neap tides. On the contrary, in very weak neap tides, neither internal bore nor arrested waves will probably happen and mixing events will be interrupted. The previous argument allows us to put forward the existence of conditions for a fortnightly cycle in biomass.

Seasonal signals are more difficult to assess. García Lafuente et al. (2002) shows the existence of an annual cycle of the inflow that peaks in late summer. Its amplitude is 10% of the mean inflow, and it is related to the annual cycle of the density differences between inflowing and outflowing waters (this cycle follows the seasonal warming of the Atlantic Water, since Mediterranean Outflowing Water is not exposed to the solar heating). The interface has an annual cycle that places it deeper in summer and shallower in late winter (February–March). The cycle in the position of the interface, which obviously has an associated cycle in the inflowing cross-area, only explains 30% of the total annual signal in the inflow. The remaining percentage is accounted for by velocity variations linked to the annual cycle of the density differences. This implies that horizontal velocities are stronger in late summer, which could favour some of the phenomena discussed here (greater shear, more mixing). On the other hand, the simultaneous sinking of the interface and the development of a seasonal thermocline will hinder the pumping of nutrients and other particles to the euphotic zone. These counteracting influences would probably obscure the biological cycle itself, and any reliable description of the seasonal cycle, if any, needs the availability of more in situ data.

3.6. The Gibraltar upwelling: concluding remarks

Mixing processes at the Sill region periodically fertilise the upper layer that enters into the Mediterranean Sea. The evidences of mixing at Camarinal allows us to present the Strait as a pulsating upwelling area because the mechanisms regulating the mixing events (formation of arrested waves and hydraulic jumps) are tidally induced. Therefore, the time when they take place is highly predictable, which is very important for evolution and ecology of organisms, as they may adapt and exploit this kind of periodicity.

Diatoms species with the "ability" of enhanced sinking rates when nutrients are limiting or long-term survival in dark environments, should be particularly suitable for these special environments. The coupling mechanisms may be inefficient, if a low percentage of diatoms is upwelled to surface waters through the conveyor belt, but diatoms are adapted to fluctuating environments and have different strategies to compensate high biomass losses (Smetacek, 1985) such as high turnover rates or resistance mechanisms including spore formation (Pitcher, 1990).

The coincidence of both the double-layer countercurrent scheme of circulation and the pulsating upwelling on the sill determines the physical structure and dynamics of the Strait. These hydrological features are closely related to the biology. In the near future the connection of the local processes taking place at the Strait to a wider scheme involving the western side of Alboran Sea should be studied.

Acknowledgements

This work was supported by the Commission of the European Communities Marine Science and Technology (MAST III) Program under Contract MAST3-96-0060 (CANIGO Project). Spanish CICYT Projects MAR96-1837 and MAR96-1950-CO2-01 supported partially our participation in non-CANIGO cruises. We also thank to the crew of the R/V *Cornide de Saavedra*, *Thalassa* and *El Investigador* for their assistance. Two anonymous referees greatly improved the manuscript. Dr. G. Parrilla made useful comments on an earlier version and is also acknowledged for his work as coordinator of CANIGO project.

References

Alpers, W., Brandt, P., Rubino, A., Backhaus, J.O., 1996. Recent contributions of remote sensing to the study of internal waves in the Straits of Gibraltar and Messina.

Bulletin of the Institute of Oceanography Monaco 17, 21–40.

Armi, L., Farmer, D.M., 1988. The flow of Mediterranean water through the Strait of Gibraltar. Progress in Oceanography 21, 1–105.

Bray, N.A., Ochoa, J., Kinder, T.H., 1995. The role of the interface in exchange through the Strait of Gibraltar. Journal of Geophysical Research 100, 10775–10776.

Bruno, M., Alonso, J.J., Cózar, A., Vidal, J., Echevarría, F., Ruiz, J., Ruiz-Cañavate, A., Gómez, F., 2002. The boiling-water phenomena at Camarinal Sill, the Strait of Gibraltar. Deep-Sea Research II 49 (19), 4097–4113.

Bryden, H.L., Candela, J., Kinder, T.H., 1994. Exchange through the Strait of Gibraltar. Progress in Oceanography 33, 201–248.

Candela, J., Winant, C.D., Bryden, H.L., 1989. Meteorologically forced subinertial flows through the Strait of Gibraltar. Journal of Geophysical Research 94, 12667–12674.

Candela, J., Winant, C., Ruiz, A., 1990. Tides in the Strait of Gibraltar. Journal of Geophysical Research 95, 7313–7335.

Dafner, E., González Dávila, M., Santana-Casiano, J.M., Sempere, R., 2001. Total organic and inorganic carbon exchange through the Strait of Gibraltar in September 1997. Deep-Sea Research I 48, 1217–1235.

Elbaz-Poulichet, F., Morley, N.H., Beckers, J.M., Nomerange, P., 2001. Metal fluxes through the Strait of Gibraltar: the influence of the Tinto and Odiel rivers (SW Spain). Marine Chemistry 73, 193–213.

Establier, R., Margalef, R., 1964. Fitoplancton e hidrografía de las costas de Cádiz (Barbate), de junio de 1961 a agosto de 1962. Investigaciones Pesqueras 25, 5–31.

Farmer, D., Armi, L., 1999. The generation and trapping of solitary waves over topography. Science 283, 188–190.

García Lafuente, J., Vargas, J.M., Plaza, F., Sarhan, T., Candela, J., Basheck, B., 2000. Tide at the eastern section of the Strait of Gibraltar. Journal of Geophysical Research 105 (C6), 14197–14213.

García Lafuente, J., Delgado, J., Vargas, J.M., Vargas, M., Plaza, F., Sarhan, T., 2002. Low frequency variability of the exchanged flows through the Strait of Gibraltar during CANIGO. Deep-Sea Research II 49 (19), 4051–4067.

Gomez, F., Echevarría, F., Garcia, C.M., Prieto, L., Ruiz, J., Reul, A., Jimenez-Gomez, F., Varela, M., 2000a. Microplankton distribution in the Strait of Gibraltar: coupling between organisms and hydrodynamic structures. J Plankton Research 22 (4), 603–617.

Gómez, F., González, N., Echevarría, F., García, C.M., 2000b. Distribution and fluxes of dissolved nutrients in the Strait of Gibraltar and its relationships to microphytoplankton biomass. Estuarine, Coastal and Shelf Science 51, 439–449.

Gorsky, G., Picheral, M., Stemmann, L., 2000. Use of the underwater video profiler for the study of aggregate dynamics in the North Mediterranean. Estuarine Coastal and Shelf Science 50 (1), 121–128.

Grasshoff, K., Erhardt, M., Kremling, K., 1983. Methods of Seawater Analysis, 2nd Edition. Verlag Chemie, Weinheim.

Harris, G.P., 1986. Phytoplankton Ecology: Structure, Function and Fluctuation. Chapman & Hall, New York, 384pp.

Jerlov, N.G., 1953. Particle distribution in the Ocean. Report of the Swedish Deep-Sea Expedition 3, 73–97.

Lacombe, H., Richez, C., 1982. The regime of the Strait of Gibraltar. In: Nihoul, J.C.J. (Ed.), Hydrodynamics of Semi-enclosed Seas. Elsevier, Amsterdam, pp. 13–73.

Mann, K.H., Lazier, J.R.N., 1991. Dynamics of the Marine Ecosystems. Biological–Physical Interactions in the Oceans. Blackwell, Boston.

Margalef, R., 1978. Life-forms of phytoplankton as survival alternatives in an unestable environment. Oceanologica Acta 1, 493–509.

Minas, H.J., Coste, B., Le Corre, P., Minas, M., Raimbault, P., 1991. Biological and geochemical signatures associated with the water circulation through the strait of Gibraltar and in the western Alborán Sea. Journal of Geophysical Research 96, 8755–8771.

Minas, H.J., Minas, M., 1993. Influence du Détroit de Gibralter sur la biogéochime de la Mediterranée et du proche Atlantique. Annales de L'Institute Océanographique Paris 69, 203–214.

Packard, T.T., Minas, H.J., Coste, B., Martínez, R., Bonin, M.C., Gostan, J., Garfield, P., Christensen, J., Dortch, Q., Minas, M., Copin-Montegut, G., Copin-Montegut, C., 1988. Formation of the Alboran oxygen minimum zone. Deep-Sea Research 35 (7), 1111–1118.

Pettigrew, N.R., Hyde, R.A., 1990. The structure of the internal bore in the Strait of Gibraltar and its influence on the Atlantic inflow. In: Pratt, J.L. (Ed.), The Physical Oceanography of Sea Straits, NATO ASI Series. Kluwer Academic, London, pp. 493–508.

Pitcher, G.C., 1990. Phytoplankton sea population of the Cape Peninsula upwelling plume, with particular reference to resting spores of *Chaetoceros* (Bacillariophyceae) and their role in seeding upwelling waters. Estuarine Coastal and Shelf Science 31, 283–301.

Reul, A., Vargas, J.M., Jiménez-Gómez, F., Echevarría, F., García-Lafuente, J., Rodríguez, J., 2002. Exchange of planktonic biomass through the Strait of Gibraltar in lake summer. Deep-Sea Research II 49 (19), 4131–4144.

Rodríguez, J., Blanco, J.M., Jiménez-Gómez, F., Echevarría, F., Gil, J., Rodríguez, V., Ruiz, J., Bautista, B., Guerrero, F., 1998. Patterns in the size structure of the phytoplankton community in the deep fluorescence maximum of the Alboran Sea (southwestern Mediterranean). Deep-Sea Research I 45, 1577–1593.

Rodríguez, J., Tintoré, J., Allen, J.T., Blanco, J.M., Gomís, D., Reul, A., Ruiz, J., Rodríguez, V., Echevarría, F., Jiménez-Gómez, F., 2001. Mesoscale vertical motion and the size structure of phytoplankton in the ocean. Nature 410, 360–363.

Smayda, T.J., 1970. The suspension and sinking of phytoplankton in the sea. Oceanography and Marine Biology Annual review 8, 353–414.

Smetacek, V.S., 1985. Role of sinking in diatoms life-history cycles: ecological, evolutionary and geological significance. Marine Biology 84, 239–251.

Stemmann, L., Picheral, M., Gorsky, G., 2000. Diel variation in the vertical distribution of particulate matter (> 0.15 mm) in the NW Mediterranean Sea investigated with the Underwater Video Profiler. Deep-Sea Research I 47, 505–531.

Sverdrup, H.U., 1953. On conditions for the vernal blooming of phytoplankton. Journal du Conseil Permanent International pour l'Exploration de la Mer 18, 287–295.

Takahashi, M., Ishizaka, J., Ishimaru, T., Atkinson, L.P., Lee, T.N., Yamaguchi, Y., Fujita, Y., Ishimura, S., 1986. Temporal change in nutrient concentrations and phytoplankton biomass in short time scale local upwelling around the Izu Peninsula, Japan. Journal of Plankton Research 8, 1039–1049.

UNESCO, 1994. Protocols for the joint global ocean flux study (JGOFS) core measurements. Manuals and Guides 29, pp. 1–170.

Wesson, J.C., Gregg, M.C., 1994. Mixing at Camarinal Sill in the Strait of Gibraltar. Journal of Geophysical Research 99, 9847–9878.